Heliyon 10 (2024) e35864

Contents lists available at ScienceDirect

Heliyon

journal homepage: www.cell.com/heliyon

Research article

Expression profile of circular RNAs in blood samples of Northern Chinese males with intracerebral hemorrhage shows downregulation of hsa-circ-0090829

Yuye Wang [a,b,1], Heyu Zhang [c,1], Yuehan Hao [a], Feng Jin [a], Ling Tang [a], Xiaoxue Xu [a], Zhiyi He [a,*], Yanzhe Wang [a,**]

[a] *Department of Neurology, Key Laboratory for Neurological Big Data of Liaoning Province, The First Affiliated Hospital of China Medical University, Shenyang, Liaoning, 110001, China*

[b] *Department of Neurology, China-Japan Friendship Hospital, Chinese Academy of Medical Sciences & Peking Union Medical College, Beijing, 100029, China*

[c] *Department of Neurology, The First Affiliated Hospital, Sun Yat-sen University, Guangdong Provincial Key Laboratory of Diagnosis and Treatment of Major Neurological Diseases, National Key Clinical Department and Key Discipline of Neurology, Guangdong, Guangzhou, 510080, China*

ARTICLE INFO

Keywords:
Intracerebral hemorrhage
Hsa-circ-0090829
Diagnostic biomarker
ceRNA
GO enrichment
KEGG pathway

ABSTRACT

Circular RNAs (circRNAs) are involved in several neurological disorders; however, the mechanisms underlying their involvement remain to be clarified. We attempted to explore the expression profiles of circRNAs and their potential functions and mechanisms in the pathogenesis of intracerebral hemorrhage (ICH) in Northern Chinese males. The microarray results showed that 50 circRNAs were significantly upregulated, while 194 circRNAs were significantly downregulated in ICH patients compared with healthy controls ($p < 0.05$). After bioinformatics analysis, a circRNA–microRNA–messenger RNA network and a protein–protein interaction network were constructed. Gene Ontology and Kyoto Encyclopedia of Genes and Genomes enrichment analyses showed that the neurotrophin signaling pathway, long-term potentiation, and the mitogen-activated protein kinase pathway are potentially implicated in ICH pathophysiology. The quantitative real-time polymerase chain reaction results revealed that hsa-circ-0090829 was significantly downregulated in ICH. The receiver operating characteristic curve analysis showed that the area under the curve of hsa-circ-0090829 between ICH and healthy controls was 0.807. Furthermore, the dual-luciferase assay showed that hsa-circ-0090829 sponged miR-526b-5p. This study reports the altered expression of circRNAs and identifies the potential functions of these circRNAs in ICH. Our results may facilitate further mechanistic research on circRNAs in ICH and provide probable novel diagnostic biomarkers and therapeutic targets for ICH.

* Corresponding author.
** Corresponding author.
E-mail addresses: hezhiyi0301@sina.com (Z. He), yanzhewangcmu@126.com (Y. Wang).
[1] **Equal contributions:** These authors contributed equally to this work.

https://doi.org/10.1016/j.heliyon.2024.e35864
Received 4 January 2023; Received in revised form 25 July 2024; Accepted 5 August 2024
Available online 8 August 2024

1. Introduction

In low- and middle-income countries, such as China, stroke is a leading cause of death and disability. With the increase in population aging and urbanization, the incidence of stroke in China is also increasing [1]. In 2017, there were 6.2 million (6.0–6.3 million) fatal cases of stroke and 132.1 million (126.5–137.4 million) stroke-related disability-adjusted life-years globally. Primary intracerebral hemorrhage (ICH) accounts for 26% of stroke cases, which causes a heavy burden on society [2]. Oppression and destruction of brain tissue by hematoma cause primary brain injury, while secondary brain injury usually involves the inflammatory response and release of clot components, which lead to neuronal death and blood–brain–barrier breakdown [3]. At present, the treatment methods for ICH mainly target primary impairment; thus, interventions targeting secondary brain injury are limited [4]. Investigating the pathophysiological development of ICH may provide a novel and more efficient way to diagnose ICH and improve clinical outcomes.

Circular RNAs (circRNAs), closed by covalent bonds during splicing, are single-stranded RNAs that were discovered decades ago. However, different from linear RNA, circRNAs do not have free 3′ and 5′ ends and cannot be measured using commonly used technology, which is dependent on the presence of poly-adenylated tails. Thus, only a small number of circRNAs have been identified. Initially, circRNAs were thought to be by-products of aberrant splicing and to have few biological functions. Powered by advanced technology in recent years, circRNAs have since demonstrated universal expression in eukaryotic cells [5,6]. Research has also revealed that the brain contains more circRNAs than other tissues, such as the lungs, liver, heart, and testes. Brain-expressed circRNAs are often conserved and have a high degree of sequence similarity among human, mouse, and even Drosophila brains [7].

There are three common mechanisms through which circRNAs exert their functions. Specifically, circRNAs function as miRNA sponges, gene transcription regulators, and protein or peptide encoders [8]. Available data reveal that circRNAs play important roles in ischemic stroke [9–12], neurodegenerative diseases [13–15], and demyelinating diseases [16–18], either by interacting with proteins or microRNAs (miRNAs) or by functioning as biomarkers. However, little is known about circRNAs and ICH pathogenesis. Considering the conservation and tissue specification of circRNAs in the brain, it is worthwhile to investigate whether circRNAs could behave as biomarkers in ICH. In addition, exploring new therapeutic targets for ICH is clinically meaningful. CircRNA expression profiles are a useful basis for further studies on this topic.

As far as we know, this is the first study to investigate the circRNA expression profiles of Northern Chinese male patients with ICH. In this study, we first utilized circRNA microarray analysis to determine the circRNA expression profile using peripheral circulating blood. We then used quantitative real-time polymerase chain reaction (qRT-PCR) for validation. Then, we performed bioinformatics analyses to explore the functions of the significantly differentially expressed circRNA, hsa-circ-0090829. The dual-luciferase assay was used to validate the circRNA–miRNA sponge interaction. Finally, a circRNA–miRNA–mRNA network was created, and the potential mechanisms underlying the effects of hsa-circ-0090829 on ICH pathophysiology were illustrated by identifying the functions of miR-526b-5p target genes. The results will allow us to better comprehend the molecular pathogenesis of ICH, as well as to better explore novel ICH biomarkers and possible treatment sites in the long term.

2. Methods

2.1. Study population

Male patients who attended the First Affiliated Hospital of China Medical University were enrolled. Nineteen patients who received a clinical diagnosis of ICH between July 2020 and December 2020 were included in this study. Thirteen healthy controls were also enrolled. From these 19 patients and 13 controls, four ICH samples and four samples from healthy controls were chosen at random for circRNA detection (Agilent Microarray). All of the samples were used to validate the differentially expressed circRNAs. The following were inclusion requirements for patients with ICH: (1) male patients aged between 40 and 80 years; (2) ICH confirmed by brain imaging (computed tomography); (3) spontaneous ICH that had not broken into the ventricle; and (4) patients who did not undergo surgical therapy. If a patient met any of the following, they were excluded: (1) secondary ICH caused by brain trauma, tumor, vascular malformation, arteritis, anticoagulant usage, or other causes; (2) severe primary disease of the circulatory, respiratory, digestive, urinary, hematological, or endocrine systems; and (3) bleeding that had broken into the ventricle. The flowchart is shown in Fig. 1.

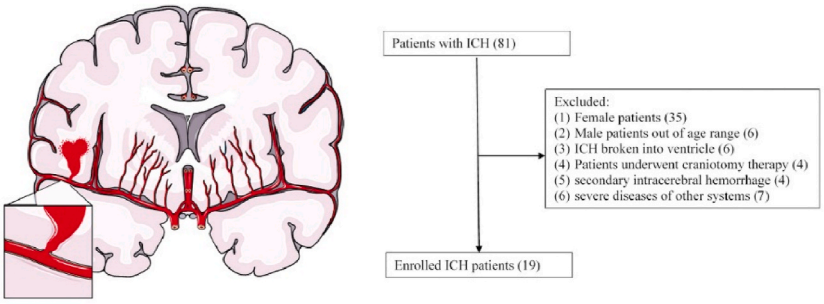

Fig. 1. Flowchart of the enrolment of patients with ICH.

Controls were healthy volunteers or patients without neurologic deficits who were matched by sex and age to the patient group. Only male participants were enrolled because we wanted to ensure the homogeneity of patients and exclude the effects of sex hormones.

2.2. Specimen collection and RNA extraction

The day after admission, blood samples were collected through venipuncture into sterile anticoagulant tubes containing ethylenediaminetetraacetic acid, and they were processed within 1 h. Following the manufacturer's instructions, total RNA was isolated from blood using RNAiso Plus reagent (Takara, Japan). All total RNA samples were stored at −80 °C until further analysis.

2.3. Construction of circRNA microarrays

The expression profile was obtained by Shanghai Personalbio technology Co. Ltd. (Shanghai, China) using the Agilent Scanner G2505C. The RNA concentration was measured using the NanoDrop ND-2000 spectrophotometer (Thermo Fisher Scientific, US). The integrity and quality of the RNA were assessed using the Agilent Bioanalyzer 2100 (Agilent Technologies, US). The QIAGEN RNeasy Mini Kit (Qiagen, Germany) was used to purify RNA. After hybridization and washing, four ICH samples and four control samples were analyzed on the circRNA chip. Significantly differentially expressed circRNA transcripts were those with P values of <0.05 and threshold values of $\geq$2-fold change.

2.4. Construction and analysis of the circRNA–miRNA-messenger RNA (mRNA) network

We created a competing endogenous RNA (ceRNA) network with hsa-circ-0090829 at the center. CircRNA–miRNA interactions were predicted using TargetScan, miRanda, and CircInteractome (https://circinteractome.nia.nih.gov/), while miRNA–mRNA interactions were predicted using TargetScan (http://www.targetscan.org/vert-72/), miRWalk (http://mirwalk.umm.uni-heidelberg.de/), and miRDB (http://mirdb.org/). The overlapping predicted genes from different websites were selected for further analysis. Then, the predicted circRNAs, miRNAs, and mRNAs were chosen to construct the network. Finally, a circRNA–miRNA–mRNA network based on the chosen circRNA and the corresponding miRNA–mRNA was created using Cytoscape.

2.5. Gene Ontology (GO) and Kyoto Encyclopedia of genes and Genomes (KEGG) pathway analyses

Biological processes (BPs), cellular components (CCs), and molecular functions (MFs) are the three perspectives from which the GO enrichment analysis explains the functions of associated genes. We were able to identify the biological pathways of the selected circRNA in the collected samples according to the analysis mentioned above. The GO enrichment and KEGG pathway analyses were performed to determine the GO terms associated with the functions of the hsa-circ-0090829-related mRNAs.

2.6. Construction of the protein–protein interaction (PPI) network

We utilized the STRING online website (https://string-db.org/) to create the PPI network. Target genes were uploaded to the STRING website, and unconnected nodes in the network were omitted. The visualization of the interaction network was directly exported from the website.

2.7. qRT-PCR

A qRT-PCR analysis of hsa-circ-0090829 was performed to further confirm the reliability of the RNA microarray results. Between 1.8 and 2.0 was the range for the absorbance at 260/280 nm. The HiScript III 1st Strand cDNA Synthesis Kit (+gDNA wiper) was used to reverse transcribe total RNA into complementary DNA (cDNA), and qRT-PCR was performed using ChamQ Universal SYBR qPCR Master Mix (Vazyme, China) in accordance with the manufacturer's instructions. Biotech & Biomedicine (Shenyang, China) created the circRNA primers. The internal control was GAPDH. The $2^{-\Delta\Delta Ct}$ method was used to quantify the circRNA qRT-PCR results. Three duplicates of each experimental reaction were carried out.

2.8. Dual-luciferase assay

293T cells (Chinese Academy of Sciences, China) were seeded onto 96-well plates and cultured overnight until 70 % confluent. The pMIR-REPORT Luciferase plasmids containing the sequences of wild-type hsa-circ-0090829 and hsa-circ-0090829 with mutant miRNA binding sites were constructed using OBiO Technology (Shanghai, China). The ratio of Firefly vector to Renilla vector to transfection reagent was 0.2 μg: 0.01 μg: 0.25 μL. Cells were then transfected with wild-type or mutant plasmids and miRNA or negative control (NC) (100 nM), respectively, using Lipofectamine 2000 (Invitrogen, US). The NC was relative to the miRNA mimic, which could not lead to overexpression of miRNA and further evaluate sequence-specific effects. Then, using a dual-luciferase reporter assay system, luciferase activity was assessed 48h after transfection (Promega, US), as quantified by the ratio of Firefly to Renilla activity.

2.9. Statistical analysis

For the microarray and dual-luciferase assay data, the *t*-test was used to compare the two groups. For the qPCR results of hsa-circ-0090829, the Kolmogorov–Smirnov test was used to determine whether the variance among the groups was normally distributed before conducting any statistical data analysis. The Mann–Whitney *U* test was used to compare the medians of the two groups. Receiver operating characteristic (ROC) curves and correlated area under the ROC curve (AUC) values were used to examine the diagnostic performance of hsa-circ-0090829. ICH was inputted as a positive outcome. *ROCR* (http://rocr.bioinf.mpi-sb.mpg.de) was used to plot the ROC curves. SPSS version 23.0 (IBM Corp., US) was utilized for the statistical analysis, while R version 4.1.0 was used for visualization. A p value of <0.05 was considered statistically significant.

3. Results

3.1. Baseline characteristics of patients with ICH and healthy controls

The baseline data of 13 healthy controls and 19 patients with ICH who participated in this study from July 2020 to December 2020 were collected. Table 1 displays the clinical characteristics of the individuals. Between patients with ICH and healthy controls, there were no significant differences in age or the prevalence of smoking, diabetes mellitus, hyperlipidemia, or hypertension.

3.2. Overview of circRNA expression profiles in patients with ICH and healthy controls

To investigate the function of circRNAs in the occurrence and development of ICH, the circRNA microarray analysis was performed to identify the differentially expressed circRNAs between patients with ICH and healthy controls. In total, 26,410 circRNAs were upregulated and 33,710 circRNAs were downregulated. When comparing patients with ICH with healthy controls, we discovered that 50 circRNAs were significantly upregulated and 194 circRNAs were significantly downregulated (absolute log2 fold change of ≥ 1, $p < 0.05$). To assess the variation and reproducibility of circRNA expression in the blood between patients with ICH and healthy controls, a volcano plot was produced (Fig. 2A). Significantly elevated circRNAs are shown by the red dots, while significantly downregulated circRNAs are represented by the blue dots.

Hsa-circ-0020173 (log2 fold change of 2.18, $p = 0.02$) and hsa-circ-0046386 (log2 fold change of -2.74, $p = 0.02$) were the top upregulated and downregulated circRNAs, respectively, when comparing ICH patients with healthy controls. The expression patterns of the top 10 circRNAs between patients with ICH and healthy controls are displayed in a hierarchical clustering heatmap (Fig. 2B). Blue signifies low relative expression, whereas red signifies high relative expression.

3.3. Validation of hsa-circ-0090829 expression and identification of novel circRNA biomarkers for ICH

The correlation analysis of RNA interactions revealed that hsa-circ-0090829 was the most suitable circRNA among the top 10 most upregulated and downregulated circRNAs based on the TargetScan score and miRanda energy. To verify hsa-circ-0090829, qRT-PCR was performed in 15 patients with ICH and 9 healthy controls. Hsa-circ-0090829 was significantly downregulated in ICH patients when compared to healthy controls, which indicated the same directional trend as was discovered in the microarray analysis ($p = 0.012$) (Fig. 3A). We conducted the ROC curve analysis to assess the potential diagnostic ability of hsa-circ-0090829 in ICH. The AUC value of hsa-circ-0090829 between ICH patients and healthy controls was 0.807 according to the ROC curve analysis ($p = 0.013$) (Fig. 3B). The Youden index reached its maximum when the sensitivity reached 0.889 and the specificity reached 0.800. Thus, hsa-circ-0090829 was considered valuable for the diagnosis of patients with ICH.

3.4. Hsa-circ-0090829 sponged miR-526b-5p

Recent studies have reported that circRNAs may serve as miRNA sponges, thus downregulating the expression of miRNA targets and upregulating the expression of mRNAs. A circRNA–miRNA–mRNA network was created from the prediction applications. The circRNA–miRNA interaction was predicted using CircInteractome (https://circinteractome.irp.nia.nih.gov/mirna-target-sites.html), TargetScan, and miRanda. The bioinformatics analysis showed that miR-486-3p and miR-526b-5p were integrated miRNAs by three *in silico* prediction tools. The predicted binding sites are shown in Table 2.

Table 1
Clinical features of the participants.

Characteristics	ICH patients (n = 19)	Controls (n = 13)	P value
Age (mean ± SD), years	56.26 ± 11.357	58.23 ± 6.894	0.582
Hypertension, n	13	5	0.149
Diabetes mellitus, n	6	4	0.868
Smokers, n	8	4	0.668
Hyperlipidemia, n	7	7	0.246

ICH, intracerebral hemorrhage.

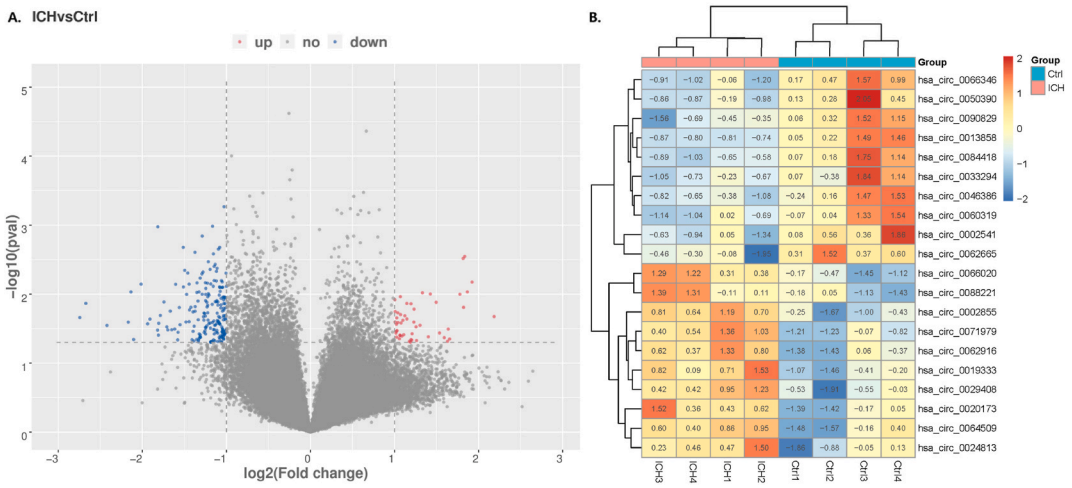

Fig. 2. Differential expression of circRNAs in the blood between patients with ICH and healthy controls. **A.** Differentially expressed circRNAs shown using a volcano plot. Fifty circRNAs were significantly upregulated, while 194 circRNAs were significantly downregulated in patients with ICH compared with healthy controls. **B.** The expression patterns of the top 10 circRNAs between patients with ICH and healthy controls shown by the hierarchical clustering heatmap. Hsa-circ-0090829 was significantly downregulated in patients with ICH.

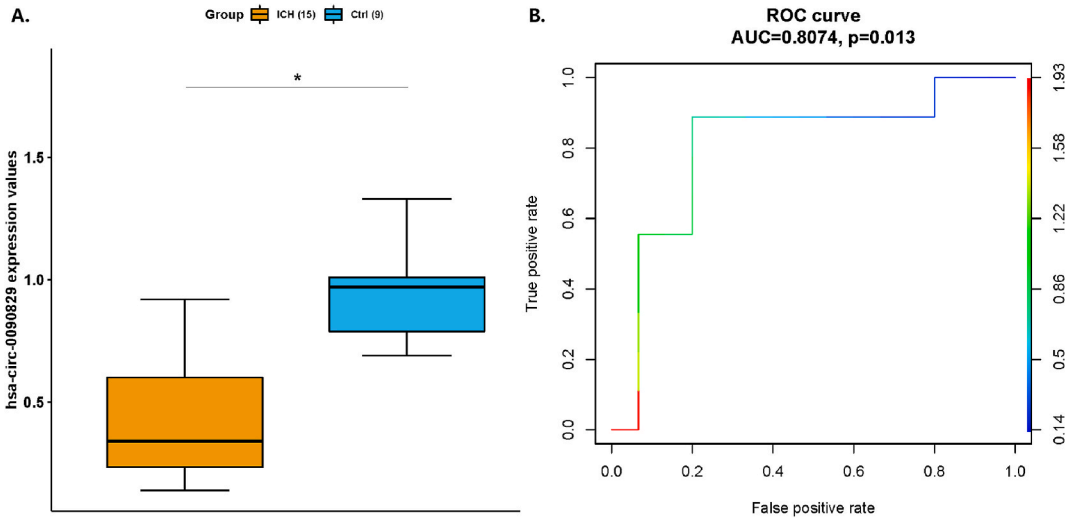

Fig. 3. Expression and ROC curve of hsa-circ-0090829. **A.** Boxplot indicating the relative expression of hsa-circ-0090829 between patients with ICH and healthy controls using qRT-PCR (*U* test *p < 0.05). **B.** ROC curve of hsa-circ-0090829 to differentiate patients with ICH from healthy controls (*p < 0.05). The X axis indicates the false-positive rate. The left Y axis indicates the true-positive rate. The right Y axis indicates the relative expression value.

Table 2
Binding site of hsa-circ-0090829 and miRNAs.

miRNA	Leftmost position of the predicted target site	Folding energy (in kcal/mol)	Heteroduplex
hsa-miR-486-3p	221	−12.90	CCCCGCTATGAGCTTCTTCT TAGGACATGACTCGACGGGGC
hsa-miR-526b-5p	223	−15.10	CCGCTATGAGCTTCTTCTCAAGGA TGTCTTTCACGAAGG-GAGTTCTC

Next, the luciferase activity in 293T cells was assessed after cotransfection with miR-526b-5p mimic or mimic NC and pMIR-REPORT Luciferase-hsa-circ-0090829 (WT) (Fig. 4A) or pMIR-REPORT Luciferase-hsa-circ-0090829 (MUT) (Fig. 4B). As shown in Fig. 4C, the miR-526b-5p mimic significantly decreased hsa-circ-0090829 (WT)-mediated luciferase activity (p = 0.016) when

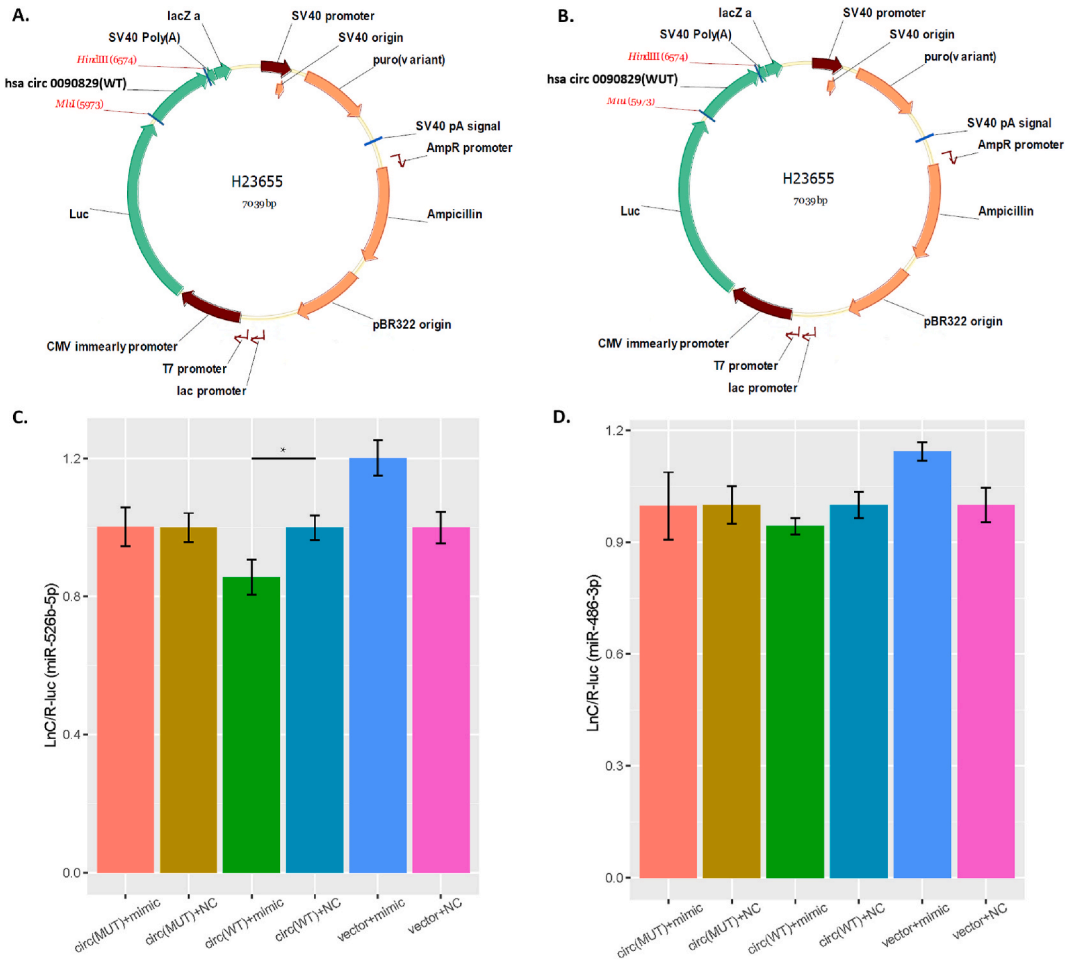

Fig. 4. Plasmid construction and results of the dual-luciferase assay. **A.** Hsa-circ-0090829 (WT) plasmid. **B.** Hsa-circ-0090829 (MUT) plasmid. **C.** The miR-526b-5p mimic significantly decreased hsa-circ-0090829 (WT)-mediated luciferase activity (T test *$p < 0.05$) compared to NC, but it had no effect on hsa-circ-0090829 (MUT)-mediated activity. **D.** The miR-486-3p mimic did not significantly decrease hsa-circ-0090829 (WT)-mediated luciferase activity.

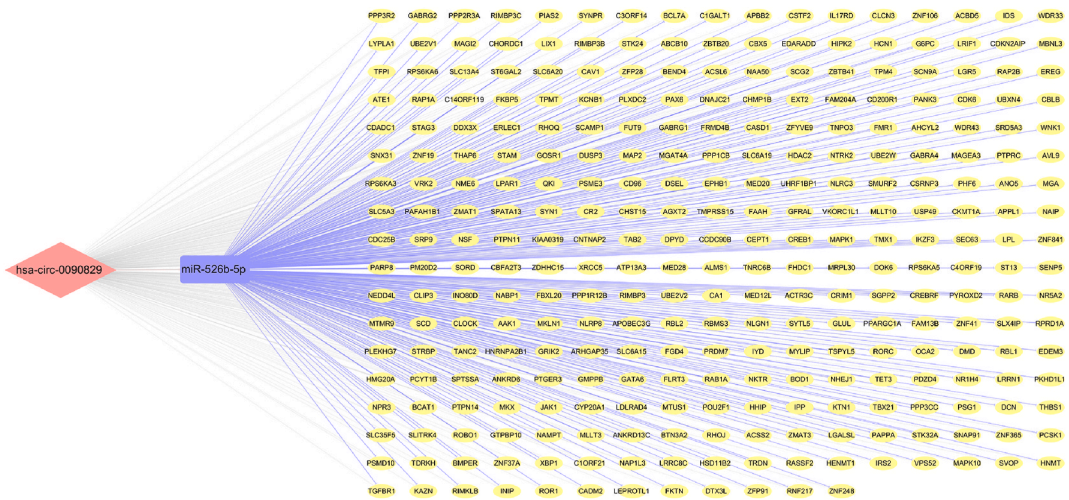

Fig. 5. Hsa-circ-0090829–miR-526b-5p–mRNA ceRNA network.

compared to NC, but it did not have an effect on hsa-circ-0090829 (MUT)-mediated activity. However, miR-486-3p mimic did not decrease hsa-circ-0090829 (WT)-mediated luciferase activity (Fig. 4D).

3.5. Construction and analysis of the circRNA–miRNA–mRNA network

The miRNA–mRNA interaction was analyzed using TargetScan, miRWalk, and miRDB. MiR-526b-5p-related mRNAs were defined as the intersection genes of the TargetScan, miRWalk, and miRDB databases. The circRNA–miRNA–mRNA network displayed the relationships among hsa-circ-0090829, miR-526b-5p, and the target genes. The network analysis results suggested that the target genes could be regulated by hsa-circ-0090829 and miR-526b-5p in cascade. The findings suggest that the possible regulatory functions of hsa-circ-0090829 occur by interactions with miR-526b-5p target genes, which may be crucial for ICH development (Fig. 5).

3.6. GO and KEGG pathway analyses

The functions and mechanisms of hsa-circ-0090829 remain undetermined. Thus, we analyzed the GO and KEGG pathway enrichment of miR-526b-5p target genes derived from the intersection genes of miRDB, miRWalk, and TargetScan. We observed that positive regulation of transcription from the RNA polymerase II promoter (BP), post-synapse (CC), and protein serine/threonine/tyrosine kinase activity (MF) were the most enriched terms. The most significantly enriched GO term was positive regulation of protein catabolism, which is related to protein metabolism. The detailed results are presented in Fig. 6A. The KEGG pathway analyses of these target genes suggested that they participate in many pathways (Fig. 6B), such as mitogen-activated protein kinase (MAPK) signaling (hsa04010), insulin signaling (hsa04910), neurotrophin signaling (hsa04722), and long-term potentiation (hsa04720).

3.7. PPI network construction

Based on the STRING database, we constructed the PPI network for the target genes, as illustrated in Fig. 7. The query proteins as well as the first shell of interactors are visually denoted through nodes of various colors. Connections between proteins, whether functional or physical, are depicted by edges. The varying thicknesses of these edges reflect different levels of confidence in the associations.

4. Discussion

Stroke, which is the second leading cause of mortality and a major contributor to disability globally, is most highly prevalent in developing countries [19]. Acute medical management for ICH includes blood pressure lowering and hemostatic agents, which are mainly symptomatic treatments [20]. Under this background, investigating the treatment of ICH according to its pathophysiology is necessary.

One study involving patients with ICH and three studies using ICH rodent models have been performed to investigate the role of circRNAs in ICH. Bai et al. implied that 229 circRNAs were upregulated and 161 circRNAs were downregulated with a fold change of >1.5 and a false discovery rate of <0.05 when comparing hypertension plus ICH with hypertension only. Three circRNAs (hsa-circ-0001240, hsa-circ-0001947, and hsa-circ-0001386) may be useful as individual or combination biomarkers for the prediction and diagnosis of ICH [21]. In a rat ICH model (intrastriatal injection of autologous artery blood), 111, 1145, and 1751 upregulated circRNAs, as well as 47, 732, and 1329 downregulated circRNAs, were detected in the cerebral cortex at 6, 12, and 24 h when compared with the sham group. Ninety-three circRNAs were elevated and 20 circRNAs were downregulated at each of these three time points [22]. A total of 11,620 circRNA transcripts were identified in rat brain tissues, of which 79 were significantly downregulated and 83 were significantly upregulated on day 7, while 95 were significantly downregulated and 84 were significantly upregulated on day 28 in the ICH group. The first 10 terms on day 28 included developmental processes, detection of chemical stimulus involved in sensory perception of smell, generation of neurons, plasma membrane-bounded cell projection, neuron projection, DNA-binding transcription factor activity, and RNA polymerase II-specific, amongst others. In the KEGG pathway analysis, the most significant

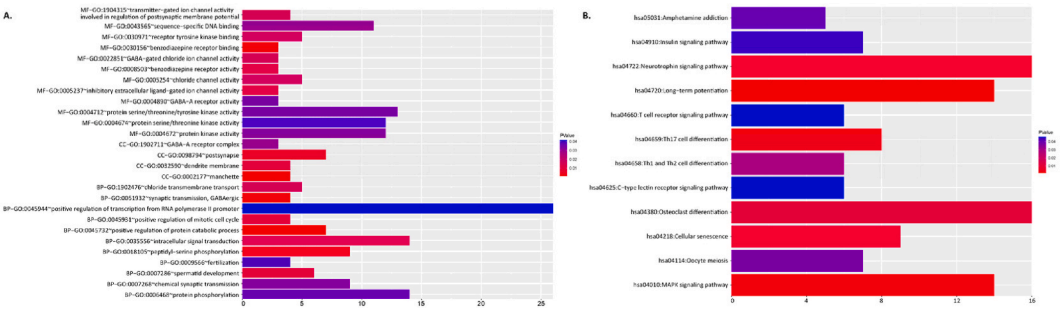

Fig. 6. GO and KEGG pathway enrichment results of miR-526b-5p target genes (*p < 0.05). **A.** GO enrichment results of miR-526-5p target genes. **B.** KEGG pathways enriched by miR-526b-5p target genes.

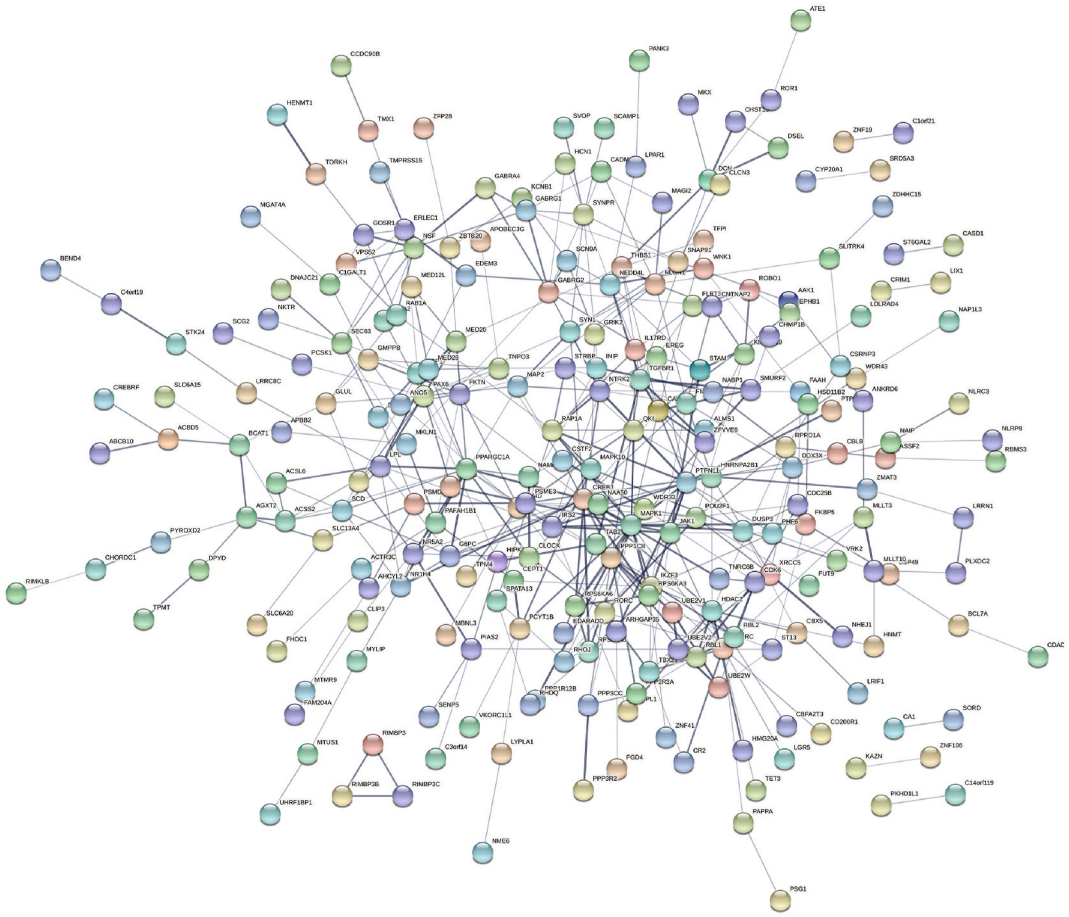

Fig. 7. PPI network of miR-526b-5p target genes.

pathways included several brain pathways, such as neuroactive ligand–receptor interactions, synaptic vesicle cycle, and the calcium signaling pathway, on both days 7 and 28 [23]. In another ICH model (type VII collagenase), there were 346 and 389 differentially expressed circRNAs at 24 and 48 h after ICH, respectively. Bioinformatics analyses showed that downregulated circRNAs were enriched in dopaminergic synapses, glutamatergic synapses, endocytosis, actin cytoskeleton regulation, MAPK signaling, and retrograde endocannabinoid signaling [24].

This is the first study to investigate the role of circRNAs in male patients with ICH compared with age-matched controls, which could eliminate the influence of sex hormones. We screened for circRNAs that were differentially expressed by microarray analysis. The chip data showed that 50 circRNAs were significantly elevated, while 194 circRNAs were significantly downregulated in patients with ICH compared with healthy controls. We reported the top 10 significantly differentially expressed circRNAs. After the RNA interaction analysis, we chose hsa-circ-0090829 for expression validation, and using qRT-PCR, we proved the downregulation of hsa-circ-0090829 in patients with ICH, which is consistent with the microarray data. Hsa-circ-0090829 has not been reported in previous studies; thus, this is a novel finding. The ROC curve analysis showed that hsa-circ-0090829 can be used as a potential diagnostic biomarker for ICH with an AUC of 0.807. It is also suggested to be a new therapeutic target through the regulation of downstream pathways. Briefly, supplementation with hsa-circRNA-0090829 can affect multiple ICH-related pathways by sponging miR-526b-5p, thereby releasing downstream target genes.

We also constructed a circRNA–miRNA–mRNA network. According to the prediction, miR-486-3p and miR-526b-5p are miRNAs that interact with hsa-circ-0090829. The dual-luciferase assay confirmed the role of hsa-circ-0090829 as the miR-526b-5p sponge. MiR-526b-5p has not been reported in previous studies related to ICH, making it another novel finding. We further identified the target genes of miRNAs using *in silico* target prediction tools. There were 301 target genes of miR-526b-5p identified using miRDB, TargetScan, and miRWalk. Based on our results and previous evidence, we suggest that hsa-circ-0090829 might be involved in the pathophysiology of ICH through the ceRNA mechanism. Downregulation of hsa-circ-0090829 might increase the content of miR-526b-5p, leading to inhibition of target mRNAs.

Finally, we performed GO and KEGG pathway analyses. MiR-526b-5p-related genes were enriched in many MFs, CCs, and BPs that are correlated with ICH. Protein serine/threonine/tyrosine kinase activity, post-synapse, and positive regulation of transcription from the RNA polymerase II promoter were the most enriched terms. Moreover, many ion channel activity-related MFs [25], as well as

protein phosphorylation and catabolism-related BPs [26], were enriched. According to the KEGG pathway analysis, target genes were mostly enriched in the neurotrophin signaling pathway. Knockdown of the p75 neurotrophin receptor promotes neuronal autophagy by inactivating the mTOR pathway [27] and reducing neuronal apoptosis [27–29] in rats with ICH. Brain-derived neurotrophic factor (BDNF) is involved in neuroplasticity and beneficially contributes to stroke recovery [30–32], and cortical BDNF mRNA expression is related to post-ICH motor impairment [30] and spatial learning and memory [33]. Transplantation of glial cell-derived neurotrophic factor improves neurological function in rats with experimental ICH [34]. In addition, neurotrophin-3 is suggested to be effective in the treatment of ICH [35]. Also, ICH impairs long-term potentiation [36,37], which is consistent with our enrichment results (hsa04720). In parallel, predicted genes were also enriched in the MAPK pathway. MAPK cascades are essential signaling pathways that control many biological activities, such as differentiation, proliferation, apoptosis, and stress responses [38], and are involved in the pathophysiology of ICH [39–41]. All of the above evidence supports our enrichment results and provides directions for future research.

Due to these restrictions, our findings should be cautiously interpreted. First, we lacked a comprehensive survey, and the sample size was relatively small. We only included males from the north as participants in our research. Thus, further study is necessary to see whether these findings may be applicable to other populations. Second, no *in vivo* or *in vitro* experiments were conducted to see if hsa-circ-0090829 contributed to ICH development. Therefore, large-scale validation studies with large sample sizes are required. It is also important to perform more investigations that include biological functional assessments, studies of females, and studies of various ethnic communities.

In summary, we reported the expression profiles of circRNAs in male patients with ICH. The results of this study suggest that hsa-circ-0090829 is downregulated in patients with ICH when compared with healthy controls, and that hsa-circ-0090829 might function as a diagnostic biomarker. We constructed a circRNA–miRNA–mRNA network to predict the interactions between target RNAs. The GO analysis revealed that target genes were enriched in ion channel activity and protein catabolism. These terms play significant roles in ICH. Moreover, the KEGG pathway analysis showed that the neurotrophin signaling pathway, long-term potentiation, and MAPK signaling might participate in the regulation of hsa-circ-0090829. This article provides a basis to study the role of hsa-circ-0090829 in ICH.

Ethics approval and consent to participate

The study was approved by the institutional ethics committee of the First Affiliated Hospital of China Medical University, China, on February 20, 2012 (approval No. 2012-38-1). The authors certify that all methods were carried out in accordance with relevant guidelines and regulations (Declaration of Helsinki). Written informed consent was obtained from all subjects.

Consent for publication

Not applicable.

Availability of data and materials

The datasets used and/or analyzed during the current study are available from the corresponding author on reasonable request.

Funding

This work was supported by grants from the National Natural Science Foundation of China (No. 82001234 to Heyu Zhang, 81971125 to Zhiyi He and No. 81901189 to Yanzhe Wang).

CRediT authorship contribution statement

Yuye Wang: Formal analysis, Methodology, Writing – original draft, Writing – review & editing. **Heyu Zhang:** Formal analysis, Funding acquisition, Methodology, Writing – original draft, Writing – review & editing. **Yuehan Hao:** Resources. **Feng Jin:** Resources. **Ling Tang:** Resources. **Xiaoxue Xu:** Methodology, Software. **Zhiyi He:** Conceptualization, Funding acquisition, Supervision. **Yanzhe Wang:** Conceptualization, Funding acquisition, Supervision.

Declaration of competing interest

The authors declare that they have no known competing financial interests or personal relationships that could have appeared to influence the work reported in this paper.

Acknowledgment

We would like to thank the nurses from the Department of Neurology and the Department of Emergency, The First Affiliated Hospital of China Medical University, for blood collection.

List of abbreviations

AUC area under the ROC curve
ceRNA competing endogenous RNA
circRNAs circular RNAs
GO Gene Ontology
ICH intracerebral hemorrhage
KEGG Kyoto Encyclopedia of Genes and Genomes
MAPK mitogen-activated protein kinase
qRT-PCR quantitative real-time polymerase chain reaction
ROC receiver operating characteristic

Appendix A. Supplementary data

Supplementary data to this article can be found online at https://doi.org/10.1016/j.heliyon.2024.e35864.

References

[1] S. Hu, et al., Stroke epidemiology and stroke policies in China from 1980 to 2017: a systematic review and meta-analysis, Int. J. Stroke 15 (1) (2020) 18–28.
[2] R.V. Krishnamurthi, T. Ikeda, V.L. Feigin, Global, regional and country-specific burden of ischaemic stroke, intracerebral haemorrhage and subarachnoid haemorrhage: a systematic analysis of the global burden of disease study 2017, Neuroepidemiology 54 (2) (2020) 171–179.
[3] R.F. Keep, Y. Hua, G. Xi, Intracerebral haemorrhage: mechanisms of injury and therapeutic targets, Lancet Neurol. 11 (8) (2012) 720–731.
[4] H. Zheng, et al., Mechanism and therapy of brain edema after intracerebral hemorrhage, Cerebrovasc. Dis. 42 (3–4) (2016) 155–169.
[5] Q. Vicens, E. Westhof, Biogenesis of circular RNAs, Cell 159 (1) (2014) 13–14.
[6] L.L. Chen, The biogenesis and emerging roles of circular RNAs, Nat. Rev. Mol. Cell Biol. 17 (4) (2016) 205–211.
[7] A. Rybak-Wolf, et al., Circular RNAs in the mammalian brain are highly abundant, conserved, and dynamically expressed, Mol. Cell 58 (5) (2015) 870–885.
[8] Y.Y. Wang, et al., The role of circular RNAs in brain and stroke, Front Biosci (Landmark Ed) 26 (5) (2021) 36–50.
[9] C. Liu, et al., Screening circular RNA expression patterns following focal cerebral ischemia in mice, Oncotarget 8 (49) (2017) 86535–86547.
[10] S.L. Mehta, G. Pandi, R. Vemuganti, Circular RNA expression profiles alter significantly in mouse brain after transient focal ischemia, Stroke 48 (9) (2017) 2541–2548.
[11] B. Han, et al., Novel insight into circular RNA HECTD1 in astrocyte activation via autophagy by targeting MIR142-TIPARP: implications for cerebral ischemic stroke, Autophagy 14 (7) (2018) 1164–1184.
[12] Y. Bai, et al., Circular RNA DLGAP4 ameliorates ischemic stroke outcomes by targeting miR-143 to regulate endothelial-mesenchymal transition associated with blood-brain barrier integrity, J. Neurosci. 38 (1) (2018) 32–50.
[13] L. Kumar, et al., Circular RNAs: the emerging class of non-coding RNAs and their potential role in human neurodegenerative diseases, Mol. Neurobiol. 54 (9) (2017) 7224–7234.
[14] R. Akhter, Circular RNA and alzheimer's disease, Adv. Exp. Med. Biol. 1087 (2018) 239–243.
[15] W.J. Lukiw, Circular RNA (circRNA) in Alzheimer's disease (AD), Front. Genet. 4 (2013) 307.
[16] J. He, et al., Exosomal circular RNA as a biomarker platform for the early diagnosis of immune-mediated demyelinating disease, Front. Genet. 10 (2019) 860.
[17] A. Zurawska, M.P. Mycko, K.W. Selmaj, Circular RNAs as a novel layer of regulatory mechanism in multiple sclerosis, J. Neuroimmunol. 334 (2019) 576971.
[18] G. Cardamone, et al., The characterization of GSDMB splicing and backsplicing profiles identifies novel isoforms and a circular RNA that are dysregulated in multiple sclerosis, Int. J. Mol. Sci. 18 (3) (2017).
[19] D. Kuriakose, Z. Xiao, Pathophysiology and treatment of stroke: present status and future perspectives, Int. J. Mol. Sci. 21 (20) (2020).
[20] I.C. Hostettler, D.J. Seiffge, D.J. Werring, Intracerebral hemorrhage: an update on diagnosis and treatment, Expert Rev. Neurother. 19 (7) (2019) 679–694.
[21] C. Bai, et al., Identification of circular RNA expression profiles and potential biomarkers for intracerebral hemorrhage, Epigenomics 13 (5) (2021) 379–395.
[22] Z. Dou, et al., Circular RNA expression profiles alter significantly after intracerebral hemorrhage in rats, Brain Res. 1726 (2020) 146490.
[23] Z. Liu, et al., Reconstruction of circRNA-miRNA-mRNA associated ceRNA networks reveal functional circRNAs in intracerebral hemorrhage, Sci. Rep. 11 (1) (2021) 11584.
[24] Y. Zhong, et al., Intracerebral hemorrhage alters circular RNA expression profiles in the rat brain, Am J Transl Res 12 (8) (2020) 4160–4174.
[25] Y.P. Zhang, H. Zhang, D.D. Duan, Chloride channels in stroke, Acta Pharmacol. Sin. 34 (1) (2013) 17–23.
[26] G. Wang, et al., Haematoma scavenging in intracerebral haemorrhage: from mechanisms to the clinic, J. Cell Mol. Med. 22 (2) (2018) 768–777.
[27] L. Wang, M. Tian, Y. Hao, Role of p75 neurotrophin receptor in neuronal autophagy in intracerebral hemorrhage in rats through the mTOR signaling pathway, Cell Cycle 19 (3) (2020) 376–389.
[28] J. Shen, et al., p75 neurotrophin receptor and its novel interaction partner, NIX, are involved in neuronal apoptosis after intracerebral hemorrhage, Cell Tissue Res. 368 (1) (2017) 13–27.
[29] T. Zhou, et al., The p35/CDK5 signaling is regulated by p75NTR in neuronal apoptosis after intracerebral hemorrhage, J. Cell. Physiol. (2019).
[30] T. Inoue, et al., Ipsilateral BDNF mRNA expression in the motor cortex positively correlates with motor function of the affected forelimb after intracerebral hemorrhage, Brain Res. 1767 (2021) 147536.
[31] M. Li, et al., Lithium treatment mitigates white matter injury after intracerebral hemorrhage through brain-derived neurotrophic factor signaling in mice, Transl. Res. 217 (2020) 61–74.
[32] J. Guan, et al., Nerve regeneration and functional recovery by collagen-binding brain-derived neurotrophic factor in an intracerebral hemorrhage model, Tissue Eng. 21 (1–2) (2015) 62–74.
[33] Y.C. Guo, et al., The expression and mechanism of BDNF and NGB in perihematomal tissue in rats with intracerebral hemorrhage, Eur. Rev. Med. Pharmacol. Sci. 21 (15) (2017) 3452–3458.
[34] L. Deng, et al., Effects of GDNF-transfected marrow stromal cells on rats with intracerebral hemorrhage, J. Stroke Cerebrovasc. Dis. 28 (9) (2019) 2555–2562.
[35] C.Y. Chung, J.T. Yang, Y.C. Kuo, Polybutylcyanoacrylate nanoparticles for delivering hormone response element-conjugated neurotrophin-3 to the brain of intracerebral hemorrhagic rats, Biomaterials 34 (37) (2013) 9717–9727.
[36] Y. Hua, et al., Y-2 reduces oxidative stress and inflammation and improves neurological function of collagenase-induced intracerebral hemorrhage rats, Eur. J. Pharmacol. 910 (2021) 174507.
[37] E. Shi, et al., Chronic inflammation, cognitive impairment, and distal brain region alteration following intracerebral hemorrhage, Faseb. J. 33 (8) (2019) 9616–9626.

[38] Y.J. Guo, et al., ERK/MAPK signalling pathway and tumorigenesis, Exp. Ther. Med. 19 (3) (2020) 1997–2007.
[39] P. Zeng, et al., Protective effects of Da-cheng-qi decoction in rats with intracerebral hemorrhage, Phytomedicine 90 (2021) 153630.
[40] F. Guo, et al., Chemokine CCL2 contributes to BBB disruption via the p38 MAPK signaling pathway following acute intracerebral hemorrhage, Faseb. J. 34 (1) (2020) 1872–1884.
[41] H. Yang, et al., Minocycline reduces intracerebral hemorrhage-induced white matter injury in piglets, CNS Neurosci. Ther. 25 (10) (2019) 1195–1206.